Investigation of the Structural and Mechanical Properties of ((82-X) Sn – XCu -18 In) % Alloy with X= 1, 2, 3, 4 and 5

A.H. Al-Hammadi [1], F.A.Ghailan [1], S.A.A. AL-Aghbari[*,1]

[1] Physics Department, Faculty of Science, Sana'a University Yemen.

*Correspond author: *Shimaav51@gmail.com*

ABSTRACT

Materials science is concerned with the development or synthesis of new materials. For this reason, our interest is focused on the fabrication of new materials, such as lead-free solder alloys. Sn-In alloys offer very low melting points and bond well with copper. This study aims to investigate the structural and mechanical properties of (82-x) Sn-18In alloys with added copper. The samples were prepared by melting technology from the high-purity (99%) elements tin, indium, and copper. XRD showed the formation of a single-phase hexagonal structure with a small copper plane, and the addition of copper decreased the particle size of the (82-x) Sn-18In. The creep test results showed that Cu-containing solder alloys exhibited significant improvements in creep resistance. However, the average activation energy decreases with copper addition from 0.322 to 0.247 eV.

CONTENTS

1. Introduction:

Since the recent emergence of environmental regulations that eliminate the use of Pb in soldering and bonding technologies in the electronic industry, the study of Pb-free alternative alloys has received significant attention[1]. Over the past decade, extensive efforts have been devoted to developing alternative Pb-free solders [2]. Sn-based alloys are among the preferred Pb-alloy substitutes in bonding technology ; because of their low melting points, low cost, good wettability, etc [3]. Currently, several types of lead-free solders, such as Sn–Ag, Sn–Cu, Sn–In, Sn–Bi, Sn–Zn, Sn–Ag–Cu, and Sn–Zn–Bi, have been developed [4].Sn–In binary alloys, particularly the Sn-20.0 wt%In alloy, have been regarded as base-alloys for low-temperature applications[5]. In addition to being lead-free, they offer very low melting points and bond well to copper, nickel, and gold substrates. They are particularly attractive for use in systems that require low-temperature

processing, such as optoelectronic devices [6]. The addition of elements such as Ag, Cu, and Zn has been introduced as an effective method to improve the mechanical strength of eutectic In–Sn alloys,and several studies have investigated the effects of Cu on In–Sn alloys [7]. For example, Duy Le Han investigated the effects of Cu addition on the microstructure and mechanical properties of an In–Sn-based low-temperature alloy. They found that the melting temperatures of the In–Sn–Cu (ISC) alloys were close to those of eutectic In–Sn alloys (115 ºC) because of the ternary reaction in the ISC alloys; Furthermore, the In–Sn-1.0Cu alloy exhibited the highest elongation of 74%, which was more than twice that of the   In–48Sn alloy. Simultaneously, the In–Sn-8.0Cu alloy exhibited the highest tensile strength of approximately 17.0 MPa, which was 1.5 times that of the In–48Sn alloy. However, the effect of Cu on the mechanical properties of Sn–In alloys has not been fully understood, especially the relationship between the microstructure of the alloy and it's mechanical properties[8]. Therefore, this study aimed to investige the effects of   Cu concentration (1,2,3,4 and 5 wt%) on the structure, tensile strength, and activation energy of the (82-x)Sn-18In alloy with Cu addition.

1.   Materials and methods
2.1. Materials preparation :
Five copper (Cu) content concentrations (1,2,3,4. and 5 wt%) were selected as doping additions to the (82-x)Sn-18In alloy. The purity of all elements of tin, induim   and copper   was approximately 99%.

 Pure elements were weighed using an electronic balance with a resolution of 1×10^{-4}g.Then the mixture was placed in a Pyrex tube. In an electric furnace at 550 ºC for 2 hours the samples were melted and then left to cool slowly at room temperature to obtain samples with fully precipitated phases, after which   all the Pyrex tubes were broken to obtain the sample. The samples were drawn in to two groups: The first group consisted of   wires of the same diameter (d =0.5 mm) and   length (L= 60 mm) for the

creep resistance test.second group consisted of small sheets for structural investigation ,after which all the samples   were polished using silicon paper and   washed in a solution of (CH_3COCH_3).

2.2. Materials investigation
   X-ray diffraction (XRD) was performed with Shimadzu EDX-720 model using CuKα radiation ($\lambda = 0.154056$ nm), and the source was operated at a voltage of 40 kV.with a constant scanning rate of 0.02/1sec. The tensile creep test was applied to all samples under four constant loads (2.4, 6.2, 8.7and 11.2) MPa at three testing temperatures (25, 40, and 80 ◦C) using a computerized vertical tensile test.

3. Results and discussion
   The findings of this study are classified into the structural and mechanical properties of [(82-x)Sn-xCu-18In] alloys   in concentrations as follows:
3.1. Structural analysis :
The X-ray diffraction patterns for (82-x)Sn-xCu-18In were obtained at room temperature. The values of 2Ө-Bragg's angle, d-spacing for the recorded peaks, and the corresponding relative intensities I/I_o (where I_o is the maximum intensity peak) for each pattern, and those obtained from JCPDS(PDF#48-1647) for 80Sn -20In, ensure that all prepared alloys were found to have a single-phase hexagonal structure with a small plane (111) of the copper. It can be seen that the copper addition changes the intensities of all Sn20-In peaks, and the position 2θ has been changed. This indicates that a shift in80Sn-20In peaks occurred. This may be attributed to the dissolution of the copper atomicsize atoms in the 80Sn-20In matrix which changed the lattice parameters and caused a shift in the80Sn-20In diffracted lines. The phases and crystal systems are shown in Fig (1).
The particle size and dislocation density were studied as a function of the Cu content, as shown in Fig (2). The particle sizes of the (82-x)Sn–18In-xCu   alloys were calculated according to

the Scherrer formula (Williamson and Hall, 1953)[9]
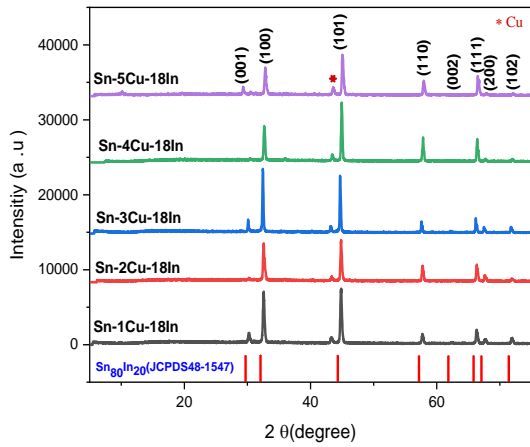
Fig(1): XRD Patterns of the Sn-XCu-18In alloys

$$D = \frac{0.9\,\lambda}{\beta\,cos\theta} \ , \tag{1}$$

where D is the particle size, β is the full width at half maximum intensity (radians), θ is the Bragg angle, and λ is the X-ray wavelength.

The average particle size values are listed in Table (1). The dislocation density was calculated according to G. K. Williamson and W. H. Hall by using[10]

$$\delta = \frac{1}{D^2} \ . \tag{2}$$

Table (1): The details of XRD analysis of Sn-In-xCu alloys.

Samples In wt.%	Particle size(D) (nm)	Dislocation density(δ) ×10⁻⁴ (nm⁻²)	Lattice distortion (ƹ)×10⁻³
81Sn-1Cu-18In	37.957	7.1	1.09
80Sn-2Cu-18In	29.220	11.8	1.34
79Sn-3Cu-18In	28.704	12.7	1.48
78Sn-4Cu-18In	34.141	7.9	1.11
77Sn-5Cu-18In	27.435	13.6	1.53

Table (1) shows that, with the addition of copper, the particle size of (82-x)Sn-18In-xCu was reduced. Copper atoms act as barriers to 80Sn-20In formation, through the solidification process that leads to the 80Sn-20In reduction ,it is clear that, as shown in Table (1) and Fig (2). Lattice distortion values were calculated

according to G. K. Williamson and W. H. Hall [10]:

$$\beta\ cos\,\theta \ = \frac{\lambda}{D} + 4\,\varepsilon\ sin\,\theta \tag{3}$$

, where D is the grain size of the 80Sn-20In matrix and ε is the local lattice distortion.
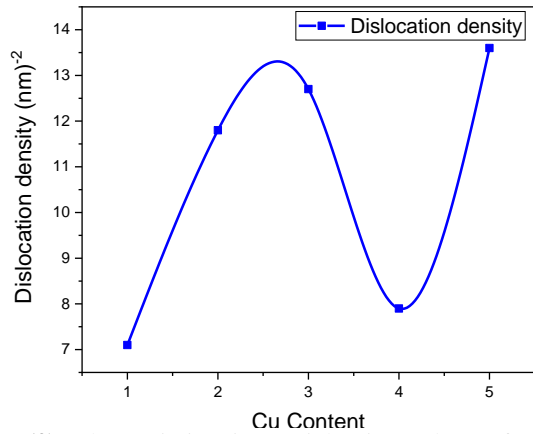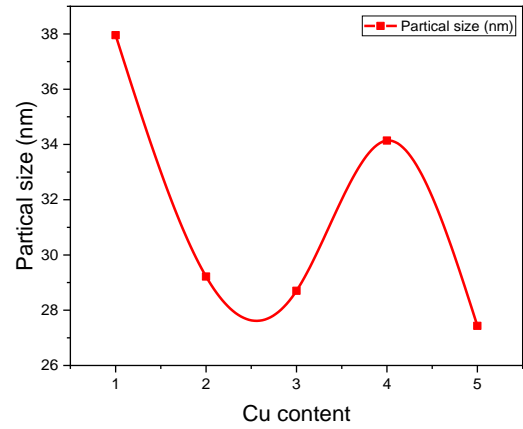

Fig (2): The variation in particle size values of SnIn with Cu-content and the variation in dislocation density values with Cu-content

3.2 X-ray density(Dₓ) and bulk density (D_b) :

The density for the samples were calculated using the relations:

$$D_x = \frac{z\,M_{wt}}{N_a\,V}$$
$$D_b = \frac{m}{V} \tag{4}$$

, where z is the number of atoms in the unit call, M_{wt} is the molar mass, N_a is the Avogadro's

number, m is the mass of the sample, and V is the volume of the sample [11].

Table(2): The X-ray density(D_x) and bulk density(D_b) of all alloys samples .

Sample no	Cu content	D_x (gm/cm^3)	D_b (gm/cm^3)
Sn-1Cu-18In	1	7.41	7.26
Sn-2Cu-18In	2	7.49	7.32
Sn-3Cu-18In	3	7.4	7.21
Sn-4Cu-18In	4	7.47	7.17
Sn-5Cu-18In	5	7.56	7.4

From Fig (3) and Table (2) it can be seen that the calculated density from the X-ray diffraction spectrum showed that it decreased with increasing Cu addition. Owing the lattice expansion in the a and c-axes with Cu addition, a slight change occurred in the (c/a) values from 0.937 to 0.944.

The maximum axial ratio value (c/a) = 0.944 was at(5.0)wt % of Cu due to the increase in   the c-axis and the contracting a-axis, which means that the cell volume decreases to 25.53 (Å^3) as shown in Table (3).
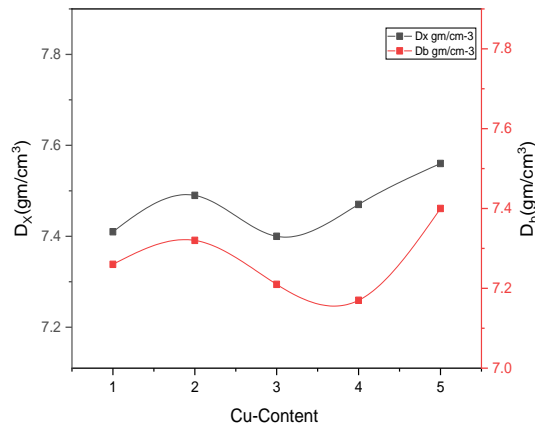

Fig (3): The X-ray density(D_x) and bulk density (D_b) as a function of Cu Content

Table (3)

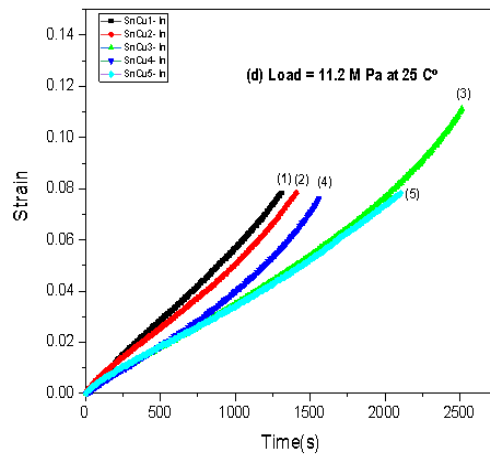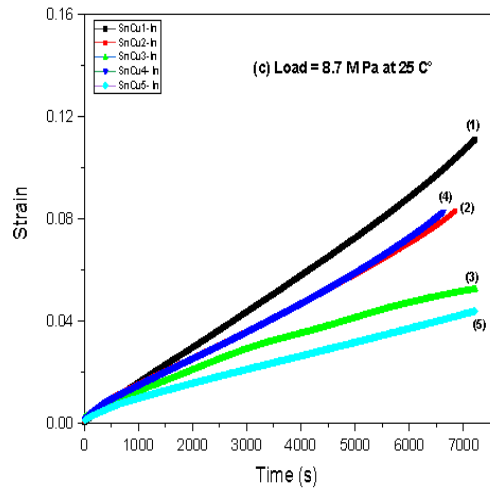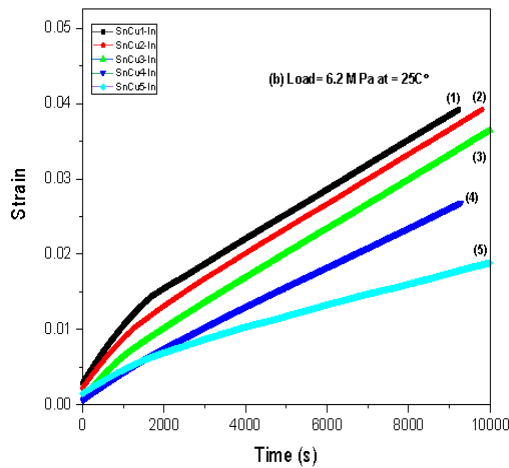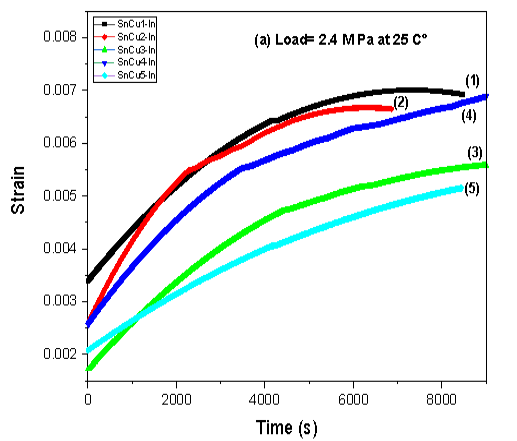| Sample no	a(nm)	c(nm)	(c/a)	Cell volume (Å^3)
Sn-1Cu-18In	3.1874	2.9875	0.937	26.328
Sn-2Cu-18In	3.1695	2.9763	0.939	25.90
Sn-3Cu-18In	3.173	2.9813	0.939	25.99
Sn-4Cu-18In	3.161	2.9763	0.942	25.75
Sn-5Cu-18In	3.1482	2.9739	0.944	25.53

3.3 Mechanical and creep behavior

The effects of different copper supplements on the mechanical properties of 82Sn–18In alloys are discussed, in terms of the stress exponent, and creep behavior. The structural stability of any alloy system is directly reflected in it's mechanical performance depending on the bonding nature of the constituent atoms [12]. Figs. (4 a, b, c, d, e, and f) indicate the strain behavior with creep time for all alloys. This test was conducted under four constant loads (2.4,6.2,8.7 and 11.2 MPa) at three working temperatures (25, 40, and 80 ◦C). For all subs(Fig. 4), it was shown that the strain rate with of the (11.2MPa) load and temperature (80 ◦C) is higher than that with the other loads (2.4, 6.2, and 8.7 MPa) and temperatures (25 and 40 ◦C), which is returned to the pressure ratio per unit area and facilitates dislocation movement at high temperatures [13].
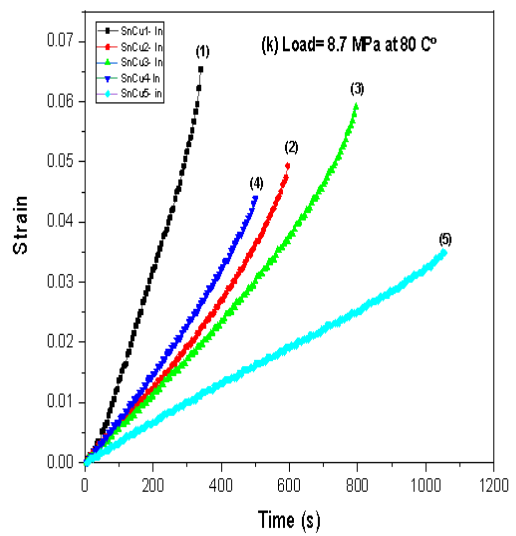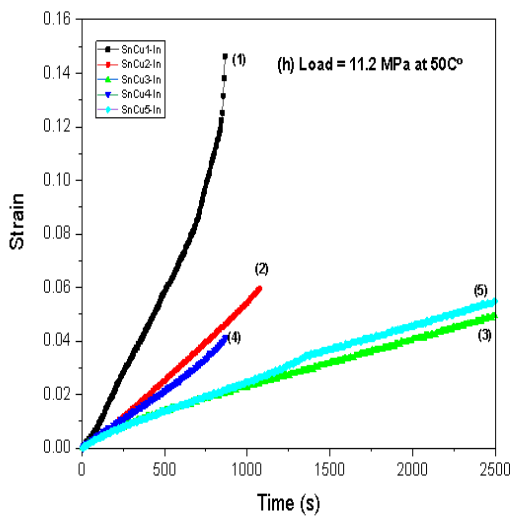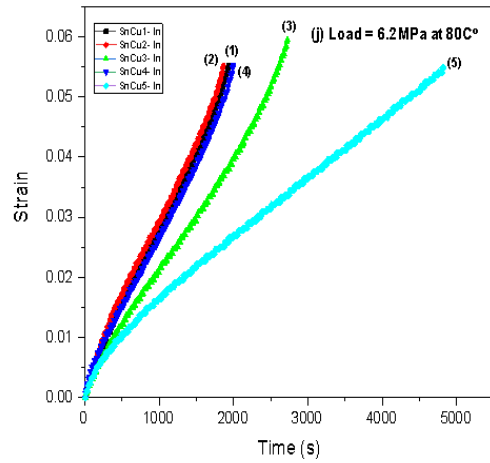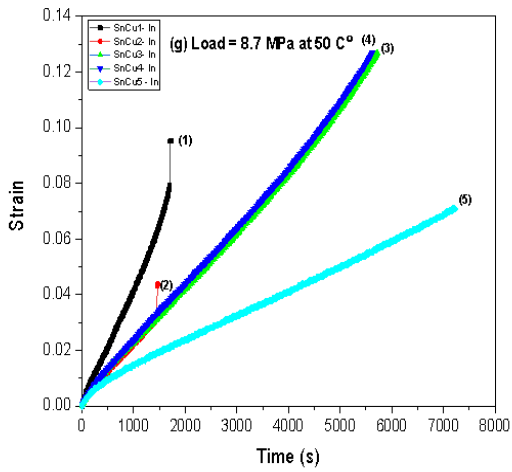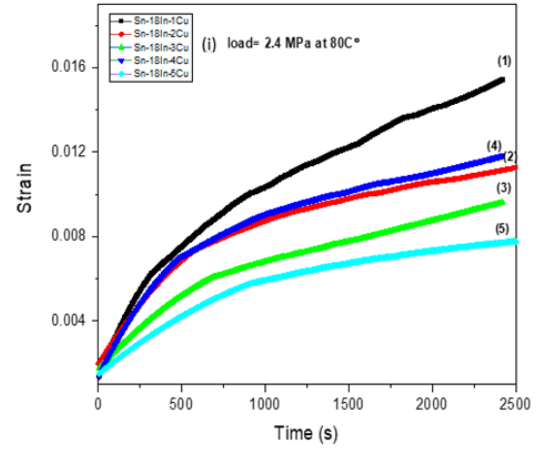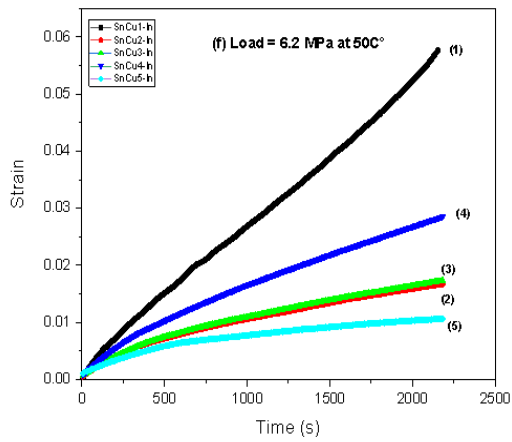
Table (4): The variation in creep rate values of Sn-18In-xCu alloys

Samples in wt.%	Loads in MPa	Creep rate (s^{-1}) Temperature 25 ºC	50 ºC	80 ºC
Sn-1Cu-In	2.4 MPa	2.489E-7	2.774E-7	1.924E-6
	6.2 MPa	3.319E-6	2.360E-5	2.4897E-5
	8.7 MPa	5.327E-6	4.20E-5	2.0971E-5
	11.2 MPa	5.70E-5	4.319E-5	2.4607E-4
Sn-2Cu-In	2.4 MPa	2.79E-7	5.824E-7	3.7401E-6
	6.2 MPa	3.09E-7	5.608E-6	2.482E-5
	8.7 MPa	1.165E-5	1.9402E-5	4.464E-5
	11.2 MPa	4.027E-5	5.741E-5	3.9658E-4
Sn-3Cu-In	2.4 MPa	2.623E-7	3.980E-7	1.666E-6
	6.2 MPa	3.623E-6	6.050E-6	2.331E-5
	8.7 MPa	1.240E-6	4.665E-5	8.557E-5
	11.2 MPa	5.85E-5	2.248E-5	6.497E-5
Sn-4Cu-In	2.4 MPa	1.262E-7	5.737E-7	1.4815E-6
	6.2 MPa	3.245E-6	1.101E-5	9.742E-5
	8.7 MPa	1.515E-5	2.133E-5	7.850E-5
	11.2 MPa	4.317E-5	1.467E-4	1.5004E-4
Sn-5Cu-In	2.4 MPa	2.439E-7	1.839E-7	1.111E-6
	6.2 MPa	3.46E-6	2.454E-6	1.810E-5
	8.7 MPa	1.448E-5	8.724E-6	8.440E-5
	11.2 MPa	3.594E-5	1.754E-5	6.6114E-5

The 81Sn-18In-1Cu alloy exhibited the lowest creep resistance (high creep rate) at all loads and temperatures; however, the 77Sn-18In-5Cu alloy exhibited the highest creep resistance (low creep rate) at all loads and temperatures, as shown in Fig. (4) and Table (3).

These improvements in creep resistance can be attributed to the distribution of copper atoms, which imped dislocation movement.

(c) Load = 8.7 M Pa at 25 C°

(a) Load= 2.4 M Pa at 25 C°

(d) Load = 11.2 M Pa at 25 C°

(b) Load= 6.2 M Pa at = 25C°

(e) Load=2.4 M Pa at 50 C°

(f) Load = 6.2 MPa at 50C°

(i) load= 2.4 MPa at 80C°

(g) Load = 8.7 MPa at 50 C°

(j) Load = 6.2 MPa at 80C°

(h) Load = 11.2 MPa at 50C°
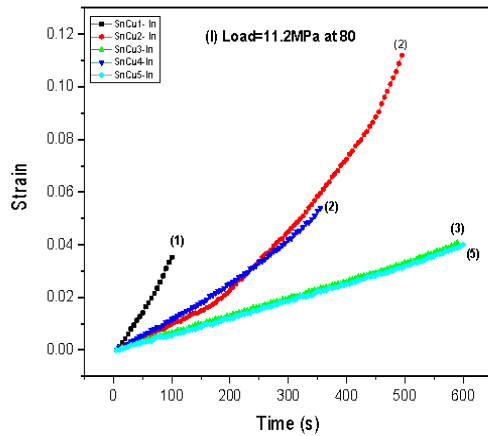

(k) Load= 8.7 MPa at 80 C°
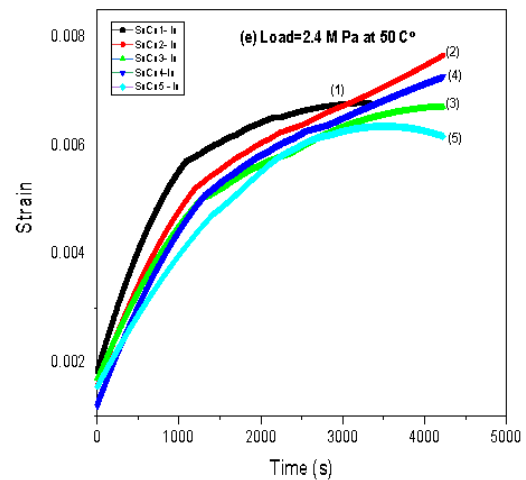
Fig (4): (a) , (b), (c),(d),(e),(f),(g) ,(h),(i),(j) , (k)and (L) Strain-time curves for Sn-18In –xCu alloys at constant loads with different temperatures

$$n= \frac{\partial \ln(\varepsilon^{\cdot})}{\partial \ln(\sigma)} \qquad (5)$$

, where $\varepsilon^{\cdot}$ is the strain rate and σ is the stress.

  The calculated (n) values with 2.4, 6.2, 8.7 and 11.2 MPa loads and different temperatures are tabulated in Table (5). indicated that by increasing the working temperature,; the stress exponent (n) decreases because of the instability of the microstructure at elevated temperatures, and this decrease in stress exponents led to an increase in the creep rate [14].

Table (5): The Stress exponent values (n) of Sn-18In-xCu alloys

Samples Cu Wt %	Stress exponent (n)		
Temperature	25 ⁰C	50 ⁰C	80 ⁰C
81Sn-1Cu-18In	3.53	3.09	2.88
80Sn-2Cu-18In	3.16	2.74	3.02
79Sn-3Cu-18In	3.02	2.25	2.47
78Sn-4Cu-18In	3.47	3.07	2.80
77Sn-5Cu-18In	2.98	2.62	2.82

   According to the above-mentioned data, the suggested creep mechanism for the 81Sn-18In-1Cu, 80Sn-18In-2Cu, 79Sn-18In-3Cu, 78Sn-18In-4Cu and 77Sn-18In-5Cu alloys at (25 and 40 ⁰C) are dislocation climb and dislocation creep at (80 ⁰C).
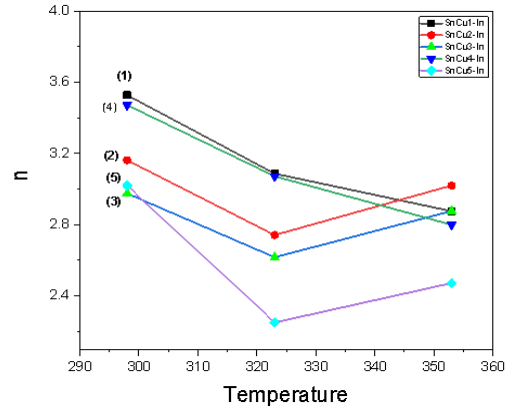

Fig. (5): The stress exponent (n) of 82Sn-18In-xCu with different temperatures.

Table (6) indicates the activation energy calculated from the relation between ln (creep rate). Moreover, the 1000/T (K $^{-1}$) of steady-state creep is shown in Fig. (6).

The activation energy obtained from the slopes of the straight lines in Fig. (4) is listed in Table (6). The results show that with the doping of copper into the (82-x)Sn-18In   alloy, the activation energy clearly changed and increased with the addition of copper . This shows that the77Sn-18In-5Cu alloy has the highest activation energy value compared to the 81Sn-18In-1Cu, 80Sn-18In – 2Cu, 79Sn-18In-3Cu,78 and Sn-18In-4Cu   alloys, which is consistent with its high creep resistance. It is also noticeable that the activation energy decreases with increasing applied stress, which means that the activation energy depends strongly on the applied stress [15].

Table (6): Activation energy (Q (eV)) of the Sn-XCu -18In

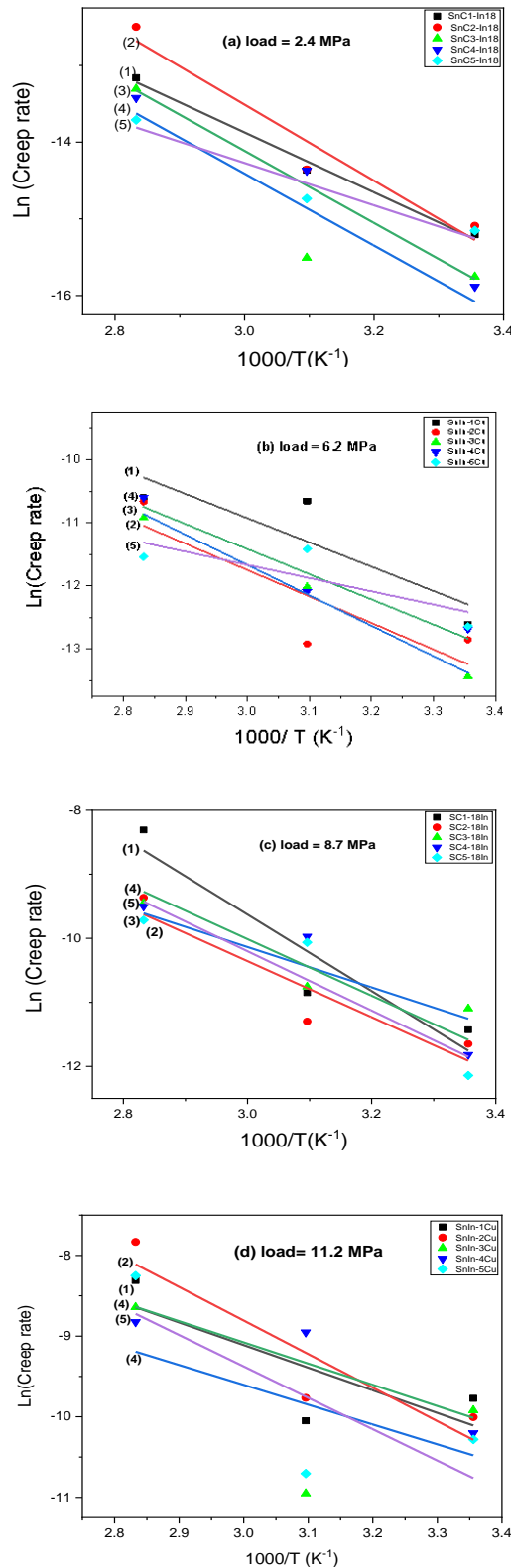| Samples in wt.%	Q (eV) under the load:				Average Q (eV)
	2.4 MPa	6.2 MPa	8.7 MPa	11.2 MPa	
Sn-1Cu-18In	0.337	0.331	0.378	0.242	0.322
Sn-2Cu-18In	0.390	0.360	0.370	0.193	0.325
Sn-3Cu-18In	0.317	0.273	0.271	0.212	0.268
Sn-4Cu-18In	0.270	0.343	0.380	0.227	0.314
Sn-5Cu-18In	0.237	0.180	0.235	0.33	0.247

Fig (6) : (a), (b), (c) and (d) The relation between Ln(ε') and 1000/T for Sn -xCu -18In Alloys at(2.4, 6.2, 8.7 and 11.2) MPa

4. Conclusion

This study investigates the (82-x)Sn-18In alloys with the additions of x wt% copper and investigates some of their structures and mechanical properties as functions of load and temperature. The X-ray diffraction analysis of the samples confirms the formation of a single phase structure with the existence of a small (111)* amount of copper. The average particle size decreases, thus the strain rateis reduced, that directly improves the mechanical performance and reliability of the alloys.

The creep results shows that the Cu-containing solder alloys exhibits a significant refinement in creep resistance. This refinement in creep resistance can be attributed to the presence of copper atoms which act as barriers to the movement of dislocations.

The activation energy (Q) values of the alloys show that the activation energy decreases with increasing the Cu added amount. It has been observed that the 77Sn-18In-5Cu alloy has the lowest activation energy value compared to the 81Sn-1Cu-18In, 80Sn-2Cu-18In, 79Sn-3Cu-18In, 78Sn-4Cu-18In alloys, which is consistent with its high creep resistance. In addition, the activation energy decreases with the increase in the applied stress, which ensures that the activation energy depends on the applied stress.

5. References

[1] A.T. Dinsdale, A. Kroupa, J. V´ızdal, J. Vrestal, A. Watson, A. Zemanova, COST Action 531-Atlas of Phase Diagrams for Lead-free Solders 1, 182, 2008.

[2] Chen S-W, Wang C-H, Lin S-K, Chiu C-N Phase diagrams of Pb-free solders and their related materials systems. J Mater Sci 18:19. doi:10.1007/s10854-006-9010-x, 2007.

[3] T. Velikanova, M. Turchanin, O. Fabrichnaya, Cu-InSn (Copper-Indium-Tin) (Materials Science International Team MSIT, 70507 Stuttgart, Germany, p. 249, 2007.

[4] Noh BI, Choi JH, Yoon JW, Jung SB. Effects of cerium content on wettability, microstructure and mechanical properties of Sn–Ag–Ce solder alloys. J Alloys Compd; 499:154–9, 2010.

[5] Lin S-K, Yang C-F, Wu S-H, Chen S-W Liquidus projection and solidification of the Sn–In–Cu

ternary alloys. J Electron Mater 37:498–506, 2008.

[6] J.W. Morris, (19930" Microstructure and Mechanical Properties of Sn-In and Sn-Bi Solders", JOM:25-27

[7] D.F. Susan, J.A. Rejent, R.P. Grant, P.T. Vianco, The solidification behavior and microstructure of in-Sn-Cu solder alloys with low Cu, in: Conference: Proposed for Presentation at the 4th International Brazing and Soldering Conference Held in Orlando, FL, 2008, pp. 1–6. [17] T. Uemura, T. Sakai, S. Sakuyama, Improvemen , 2009.

[8] D. Le Han," Effect of Cu addition on the microstructure and mechanical properties of In–Sn-based low-temperature alloy", Materials Science & Engineering, http://www.elsevier.com/locate/msea, 2021.

[9] B.D. Cullity, Elements of X-Ray Diffraction, Addison-Wesely, 1978, p. 248. Reading, 1978.

[10] G. Williamson, W. Hall, X-ray line broadening from filed aluminium and wolfram, Acta Metall. 1,22–31, 1953.

[11] F. Hussain, F.Tuamaa,"Synthesis of Nano compound (Ba1-xSrx TiO3) by Sol-Gel Method and study it's Structural Properties", Ibn AL-Haitham j.for pure &Appl.Sci, ,2016.

[12] A. Inoue, H.S. Chen, J.T. Krause, T. Masumoto, M. Hagiwara, Young's modulus of Fe-, Co-, Pd- and Pt-based amorphous wires produced by the in-rotating-water spinning method, J. Mater. Sci. 18 ,2743–2751, 1983.

[13] J. Cai, J. Lin, J. Wilsius, Modelling phase transformations in hot stamping and cold die quenching of steels, in: Microstructure. Evol. Met. Form. Process., Elsevier, pp. 210–236,2012.

[14] A.A. El-Daly, Y. Swilem, A.E. Hammad, Creep properties of Sn–Sb based lead-free solder alloys, J. Alloys Compd. 471 (1–2) 98–104,2009.

[15] C.M.L. Wu, M.L. Huang, Creep behavior of eutectic Sn-Cu lead-free solder alloy, J. Electron. Mater. 31 (5) 442–448, 2002.